RSC Advances

ROYAL SOCIETY OF CHEMISTRY

www.rsc.org/advances

Preparation of a magnetic responsive immobilized lipase-cellulose microgel catalyst system: Role of the surface properties of the magnetic cellulose microgel

Shilin Liu*, Ya Zhu, Wei Li, Yan Li, Bin Li

College of Food Science & Technology, Huazhong Agricultural University, Wuhan, Hubei, 430070 (China)

*Corresponding author: slliu2013@mail.hzau.edu.cn (S. Liu).

Abstract

Surface modification of the magnetic cellulose particles has been conducted by using AEAPS, the modified magnetic cellulose particles were then used for the immobilization of lipase for catalysis reaction. The highest specific activity for AEAPS modified magnetic cellulose scaffold was increased to about 30 folds than that of the free lipase without supports. Furthermore, the reusability of the immobilized lipase on AEAPS modified magnetic cellulose particles was also improved, the relative activity of the ARCM-2 and AMRCM1-2 after being reused for 5 times still remained 72.8% and 71.2%, respectively. Moreover, the immobilized lipase on AEAPS modified magnetic cellulose particles was easily recovered without significant decrease in the specific activity. The immobilization of lipase on AEAPS modified magnetic cellulose particles led to the improvement in stability of activity and reusability for non-aqueous transesterification.

Key words: cellulose; lipase; immobilization; magnetic scaffold

Introduction

The immobilization of enzymes has been extensively studied for the creation of a stable biocatalyst with high enzyme loading, retained or improved catalytic activity, and easily recovered and reused.[1-3] Different methods have been proposed for the immobilization of enzyme molecules, and three main strategies proposed were physical adsorption to a solid supports,[4] covalent attachment and lately cross-linking of enzyme,[5] and polymer entrapment.[6] In such approaches, a variety of materials including polymeric,[7-9] inorganic surfaces,[10-13] colloidal and powder materials has been used.[14-17] It indicated that porous structured supports have significant advantage for their the high surface areas together with the ability to encapsulate enzymes, especially, porous structured materials from biomaterials is of great of interest for its nontoxic, biocompatibility and chemical stability.[18-20]

Cellulose is the most abundant natural material with significant properties of biodegradability, and biocompatibility, it is also a very promising raw material in chemical and biological industries.[21,22] However, the potential material has not been fully exploited for its difficulty in dissolution by using conventional solvents, which was correlated to the strong inter- and intra-molecular hydrogen bonding in the macromolecules.[23-25] We have put an intensive research on cellulose dissolving and construction of functional cellulose materials from the developed solvents. In our previous work, aqueous solvents containing alkaline and urea have been developed for cellulose dissolving.[26] The regenerated cellulose materials prepared from LiOH/urea or NaOH/urea aqueous solution had porous structure, which could be

used as scaffolds for the in-situ synthesis of inorganic nanoparticles,[27] or incorporation of curable prepolymers for the construction of functional cellulose materials,[28] or in situ polymerization of conductive polymer monomer in the scaffolds.[29] It indicated that the porous structured microstructure of the cellulose scaffolds could provide a favorable reaction environment, allowing for the effective diffusion of the reactants. Therefore, cellulose scaffold was expected to serve as a versatile support material and an effective microstructured reactor site for various catalysts, including enzymes. Inspired by our previous research results, in this work, porous structured cellulose microspheres were prepared from aqueous LiOH/urea solution, and then magnetic $CoFe_2O_4$ nanoparticles were synthesized in situ in the cellulose microspheres for the preparation of magnetic responsive cellulose materials. The obtained magnetic cellulose microspheres were used as supports for the immobilization of lipase. The highest specific activity for the lipase immobilized on magnetic cellulose microspheres was increased about 7 folds. While for the magnetic cellulose microspheres after being modified with AEAPS, the highest specific activity was increased to about 30 folds than that of the lipase without supports. Furthermore, the reusability of the immobilized lipase on AEAPS modified magnetic cellulose microspheres was also improved, the relative activity of lipase immobilized on RCMs and MRCMs was only 10.4 % and 29.7% after being reused for 5 times, respectively, while for the ARCM-2 and AMRCM1-2, the relative activity still remained 72.8% and 71.2% after being reused for 5 times, respectively. Moreover, the immobilized lipase on AEAPS modified magnetic cellulose microspheres was

easily recovered without significant decrease in a specific activity. Thus, the immobilization of lipase on AEAPS modified magnetic cellulose microspheres led to the improvement of activity and reusability for non-aqueous transesterification, without notable loss of selectivity.

Experimental section

Material Native cellulose (cotton linter pulp, α-cellulose ≥ 95%) was provided by Hubei Chemical Fiber Co. Ltd. (Xiangfan, China), the viscosity-average molecular weight (M_η) was about 1.07×10^5 in cadoxen at 25 ^oC. N-3-(Trimethoxysilyl) propyl ethylenediamine, lipases (100000 U/g), DL-1-phenyl ethanol, vinyl acetate and brilliant blue G250 were purchased from Aladdin Reagent Database Co. Ltd (Shanghai, China). Other chemicals with analytical grade were purchased from the Sinopharm Chemical Reagent Co. Ltd (Shanghai, China).

Preparation of Cellulose Microspheres and Magnetic Cellulose Microspheres

The freezing-thawing method was used for cellulose dissolving. Briefly, cotton linter pulp (Native cellulose) was dispersed in aqueous lithium hydroxide/urea solution (4.6 wt%/15.0 wt%), and then put it in a refrigerator at -20 ^oC, after it has been frozen, took it out and thawed at room temperature to obtain cellulose solution (5 wt%). The resultant cellulose solution was subjected to centrifuge to eliminate some bubbles in the viscous solution. After removal of the bubbles by centrifugation, cellulose solution was added into a well-mixed suspension containing 200 ml of paraffin oils, 5g of Span 80 and 1 g of Tween 80 under mechanical stirring for 3 h. Then, dilute hydrochloric acid (10%) was subsequently added to neutralize the alkali.

After removing the liquid paraffin, the regenerated cellulose microspheres, coded as RCMs, were washed with deionized water and hot ethanol to get rid of the residual paraffin oils and surfactant thoroughly. $FeCl_3{\cdot}6H_2O$ and $CoCl_2{\cdot}6H_2O$ were dissolved in distilled water under stirring at ambient temperature (molar ratios of Co^{2+}/Fe^{3+} = 0.5). RCMs were added into the solution for 24 h and then put them in ammonia gas atmosphere for 5 h and subsequently treated with 1 M NaOH aqueous solution. The MRCMs prepared from $CoCl_2$ with concentration of 0.02, 0.04, 0.06 and 0.08 mol/L were coded as MRCM-1, MRCM-2, MRCM-3, MRCM-4, respectively.

Modification of Regenerated Cellulose Microspheres with AEAPS

Briefly, RCMs and MRCMs-1 were added to a mixture of N-3-(Trimethoxysilyl) propyl ethylenediamine (AEAPS) in 80% ethanol and then reacted at ambient temperature for 5 h. The modified RCMs and MRCM-1 were obtained by magnetic separation and washed with ethanol and distilled water. The modified RCMs and MRCM-1 prepared from AEAPS with concentration of 0.025, 0.05, and 0.1 mol/L were coded as ARCM-1, ARCM-2, ARCM-3 and AMRCM1-1, AMRCM1-2, AMRCM1-3, respectively.

Immobilization of Lipases

The lipases immobilization was carried out as follows. Firstly, 200 mg lipases were dispersed in 20 mL 0.05 mol/L phosphate buffers (pH 7.0). Then the activated magnetic carriers were mixed with lipases solution and then shaken at 37 ^{o}C for 12 h at 200 rpm. After separating the modified cellulose microspheres, the eluate was collected and coded as E1. Then the separated cellulose microspheres were put into

phosphate buffer and shaken at 37 ^{o}C for 24 h at 200 rpm to remove the noncovalent-coupled enzymes on the supports, and the eluate was also collected and coded as E2. The amount of lipases in E1 and E2 was calculated according to the Coomassie Brilliant Blue G-250 method.[30] Bovine serum albumin (BSA) was used as the standard. As a result, the amount of immobilized lipases in the cellulose microsphere scaffolds could be calculated by using the following formula:

$$A_I\ (mg) = 200 - (A_{E1} + A_{E2})$$

Where A_I was the amount of immobilized lipases, A_{E1} and A_{E2} were the amount of lipases in E1 and E2, respectively.

Characterization

The microstructure of the microspheres was characterized by using field emission scanning electron microscope (SEM) (Hitachi S4800, Japan). Transmission electron microscopy (SEM) tests were carried out with a TEM (JEOL-1010) apparatus. Wide-angle X-ray diffraction (XRD) measurement was performed with a XRD diffractometer (D8-Advance, Bruker, USA). The patterns with Cu Kα radiation at 40 kv and 30 mA were recorded in the region of 2θ from 5 to 70^{o}. Samples were ground into powders and dried in vacuum oven at 60 ºC for 48 h. Thermal gravimetric analysis (TGA) was performed by using a thermogravimetric analysis (Netzsch, German). About 10 mg of the samples was placed in a platinum pan and the test temperature ranged from 293 to 973 K at a rate of 10 K/min in air atmosphere. Fourier transform infrared (FT-IR) spectra were carried out with Nicolet 6700 spectrometer equipped with a Smart-iTR attenuated total reflectance attachment.

Nitrogen adsorption measurements were performed with a Quantachrome NOVA 4200e (USA), Brunauer-Emmett-Teller (BET) and Barrett-Joyner-Halendar (BJH) analysis were performed with the autosorb program (Quantachrome). BET analysis was carried out for a relative vapor pressure of 0.05~0.3 at 77 K. BJH analysis was performed from the desorption branch of the isotherms. The magnetic properties of the composite microspheres were evaluated with a superconducting quantum interference device (SQUID, MPMS XL-7, QUANTUM DESIGN, USA) at 298 k, and the hysteretic loop was obtained in a magnetic field that varied from -7 to +7 T. The bulk density of the microspheres was obtained by measuring the volume and weight of carved microspheres. The porosity (P_r) was calculated by using the formula: $P_r = (1 - \rho_m/\rho_t) \times 100\%$, and ρ_m was the bulk density of the final product and ρ_t was the combined density of the $CoFe_2O_4$ and cellulose at a specified ratio.

Lipases Activity Assay

The determination of lipases activity was conducted according to the previous reports.[31,32] Transesterification was carried out at 25 °C in screw-capped tubes containing 8 ml of dodecane with 500 mM DL-1-phenyl ethanol with vinyl acetate. The reaction began by adding 10 mg/L lipases or immobilized enzyme containing the same protein amount to the reaction tubes shaken by rotation. Per U of enzyme (esterification) viability was defined as per μmol of phenylethyl acetate produced per min and calculated as follows:

$$\text{Viability}\ (\text{U}/\text{mg}) = \frac{\text{k}C_2A10^6}{TA_2mM}$$

Where k was the correction factor, calculated by the peak area of standard samples,

and its formula was $k = C_1A_2/C_2A_1$. A_1 and C_1 stand for the peak area and mass of the target product phenylethyl acetate, respectively. A_2 and C_2 were for the peak area and mass of internal standard dodecane, respectively. T was the transesterification time (min). A and m were the peak area and mass of the enzyme in sample, respectively. M was the molecular weight of the target product R-acetate-1-phenylethyl. Besides, the specific activity was calculated as follows.

$$\text{Specific activity (U/g)} = V/m$$

Where V was the viability of lipases, and m was the amount of protein enzyme in sample.

Results and discussion

The process for the preparation of AMRCMs and the usage for lipase immobilization were shown in scheme 1. Cellulose microsphere prepared from aqueous LiOH/urea solvent had porous structure, as it was shown in Fig 1. The porous structure was resulted from the phase separation of the cellulose solution during the regeneration process, cellulose-rich and solvent-rich regions were formed when the cellulose solution was immersed into the non-solvent of cellulose, and the solvent-rich regions contributed to the formation of the pores. The obtained cellulose micropsheres had porosity about 94%, and the S_{BET} was about 109 $m^2 \bullet g^{-1}$. In the process of preparing magnetic $CoFe_2O_4$/cellulose microspheres, the $CoFe_2O_4$ precursor ions (Fe^{3+} and Co^{2+}) could be readily impregnated into the cellulose matrix through the pores and interacted with cellulose matrix via electrostatic interaction. After being treated with NaOH, the color of the cellulose microspheres turned into

brown, indicating that the inorganic particles had been synthesized in the cellulose matrix in situ.

The loading of inorganic magnetic components in the cellulose microspheres had an obvious influence on the microstructure, as it was shown in Fig 2. The shape of the magnetic cellulose microspheres was regular sphere and the mean diameter was about 300 μm, and there was a slightly decrease in the particle size when compared with that of pristine cellulose microspheres, it would be ascribed to the synthesized inorganic particles in the cellulose matrix, which increased the interaction of cellulose matrix and inorganic components. Therefore, the magnetic microspheres exhibited relatively denser structure than that of pristine cellulose microspheres. The cross-section images of the magnetic cellulose microspheres were shown Fig 3, the magnetic cellulose microspheres constituted porous structure in the inner parts, and the specific surface area of the composite microspheres ranged from 97 to 66 m^2/g with the increasing the concentration of $CoFe_2O_4$ precursor solution from 0.02 to 0.08 mol/L, as it was shown in Table 1, and the obtained magnetic cellulose microspheres with high surface area had great potential application in engineering field.

In order to further clarify the inorganic components in the magnetic cellulose microspheres, TEM test was carried out by ultrathin sectioning of resin-embedded magnetic cellulose microspheres, and followed by removing of the resin on the copper grid. Fig 4 shows the images of the magnetic cellulose microspheres. A large amount of inorganic nanoparticles were dispersed in the cellulose matrix. The

particle size of the $CoFe_2O_4$ nanoparticles was less than 10 nm and it increased slightly with the increasing the precursor contention. As discussed above, the incorporated Co^{2+} and Fe^{3+} ions were readily bound to cellulose nanofibrils via electrostatic interactions between the electron-rich oxygen atoms in the cellulose macromolecules and the electropositive metal cations, the Co^{2+} and Fe^{3+} ions were anchored tightly to the cellulose nanofibrils. When it was treated with NaOH solution, $CoFe_2O_4$ nanoparticles were synthesized in situ in the cellulose scaffolds. The cellulose scaffolds enhanced the formation of $CoFe_2O_4$ nuclei and preventing the particles from overgrowth, leading to the homogeneously distribution of $CoFe_2O_4$ nanoparticles in the cellulose matrix. The content of the inorganic nanoparticles increased from 4.63 to 15.28 wt% with the increasing the concentration of precursor solution from 0.02 to 0.08 mol/L. Our previous works indicated that the porous structured cellulose scaffolds was a promising template for the in situ synthesis of inorganic nanoparticles with particle size in 20 nm, and the concentration of the precursor had an influence on the content but little on the particle size of the resulted inorganic nanoparticles.[27,28]

The room-temperature magnetization hysteresis loops of the magnetic cellulose microspheres were shown in Fig 5. The forward and backward magnetization curves of the magnetic cellulose microspheres were similar. All of the curves went through zero magnetization point at $H = 0$. The absence of hysteresis and coercivity was characteristic of superparamagnetic behavior.[33, 34] It was well known that magnetic particles with particle size lower than the critical particle size could be called single

domains. As the particle size continued to decrease below the single domain value, the particles exhibited superparamagnetic properties. This result indicated that the particle size of the prepared $CoFe_2O_4$ nanoparticles in cellulose matrix was small. The magnetization of the magnetic cellulose microspheres did not exhibit saturation even at magnetic field strength as high as 20 kOe, it would be ascribed to the rotation of the magnetic moment depending on the magnetic field. Moreover, the magnetic cellulose microspheres had novel magnetic responsibility. They could move toward to the magnet direction quickly when put a magnet near to them, demonstrating that the magnetic cellulose microspheres possessed novel magnetic properties and had potential application in magnetic field-assisted manipulation.

The magnetic cellulose microspheres were used as supports for lipases immobilization as a model system to demonstrate the applications in the field of biocatalysis. The protein content loaded on the microspheres and specific activities of the free and immobilized lipases were summarized in Table 1. The amount of immobilized lipases on pure cellulose microspheres was about 0.195 mg/g, while for the magnetic cellulose microspheres, the amount of immobilized lipases increased from 0.33 mg/g for MRCM-1 to 0.563 mg/g for MRCM-3, and then deceased to 0.313 mg/g for MRCM-4, as it was shown in Fig 6. Correspondingly, the specific activity for the RCM was 0.143, and it decreased from 0.094 for MRCM-1 to 0.048 for MRCM-3, and then increased to 0.051 for MRCM-4, while for the free lipase without supporting matrix had a low specific activity (0.013). It has been reported that free lipase was easily aggregated in non-polar solvent, leading to a poor specific

activity. The immobilized lipase on the biosupport had an obviously increase in the specific activity, and it was increased to about 10 times than that of the lipase without supports. While for the magnetic cellulose supports, the specific activity of the lipase decreased when compared it with that of pristine cellulose microsphere supports, while the content of the encapsulated lipase in the magnetic cellulose supports was higher than that in the cellulose microsphere supports. It would be ascribed to the specific surface properties of the magnetic cellulose microspheres, with the incorporation of magnetic components in the cellulose matrix, the interaction between the lipase and the supports increased, and the immobilized lipase could penetrate into the inner structure and increased the bounded content of lipase in the magnetic cellulose microspheres, therefore, it was difficult for the substrates to interact with the lipases that penetrated in the inner section of the magnetic cellulose matrix, which resulted in negative effects on the specific activity of the lipases.

In order to further increase the specific activity of the magnetic cellulose microspheres supported lipases, the surface modification of the magnetic cellulose supports was carried out. Amino group modified magnetic cellulose supports was prepared via silane hydrolysis in ethanol-water medium in the presence of magnetic cellulose microspheres. After modification of the surface of magnetic cellulose microspheres, the amino functionalized supports could increase the interaction of the supports and the lipases. Fig 7 shows the FT-IR spectra of RCMs, ARCM-2, MRCM-1, and AMRCM1-2. The peaks at 3700-3200 cm^{-1} were for the O-H flex vibrations of cellulose, 1060 cm^{-1} was for the C-O bending vibrations of the ether

bond in cellulose molecules and 1157 cm^{-1} was correlated to the C-O antisymmetric bridge stretching.[35,36] According to the spectra of ARCM-2 and AMRCM1-2, the peak at 1575 cm^{-1} attributed to the $-NH_2$ bending vibrations, which verified the successful silylation modification by AEAPS. The peak for secondary amine groups in AEAPS and the H-O-H bending of the absorbed water was overlapping at 1650 cm^{-1}. The broad absorption peak around 1150 cm^{-1} was assigned to Si-O-C bond. The N1s spectra of the cellulose microspheres and magnetic cellulose microspheres after being modified with AEAPS were shown in Fig 8. The weak peak at 399.3ev was assigned to $–NH_2$.[37] Combined with the FT-IR and XPS data, it indicated that the microspheres were modified with AEAPS successfully. After being calcined at 800 oC in air atmospheres by using TGA, the residue content of ARCM-1, ARCM-2, and ARCM-3 was 3.65, 5.55 and 6.28 wt%, respectively. And the residue content of AMRCM-1, AMRCM-2 and AMRCM-3 was 6.22, 7.58 and 8.74 wt%, which was further verified the successful modification by AEAPS.

Fig 9 shows the surface morphologies of the RCM and MRCM-1 with and without the modification with AEAPS. The surface morphology of the microspheres changed after the modification with AEAPS, and the porous structure of the microspheres was disappeared, the porosity for the RCM decreased from 97 ± 5% to 65 ± 5% for ARCM-3, while it decreased from 96 ± 5% for MRCM-1 to 63 ± 3% for AMRCM1-3. Correspondingly, the S_{BET} of the RCM and MRCM-1 decreased with the modification of the surface by using AEAPS, and the specific area decreased with the increasing the concentration of the reacted AEAPS, as it was shown in the

Table 1. Thus, combined with the results from the FT-IR and TGA analyses, it suggested that the surface of the cellulose and magnetic cellulose microspheres had been modified by using AEAPS. The specific activity of lipase on the pristine cellulose microspheres was about 0.143U, and it increased to 0.399U for ARCM-1. With the increasing the concentration of the used AEAPS for the modification of RCM, the specific activity for the immobilized lipase increased correspondingly, as it was shown in Fig 10a. It was worth noting, the specific activity for the immobilized lipase on ARCM-3 was about 30 times than that of the free lipase. While for the AEAPS modified magnetic cellulose microspheres, the specific activity for the immobilized lipase also increased obviously when compared with that of the magnetic cellulose microspheres without modification with AEAPS, and the highest specific activity for AMRCM1-2 was increased to about 30 times than that of the lipase without supports. It would be resulted from the introduced $–NH_2$ group from the AEAPS that contributed to the improvement of lipase activity for non-aqueous transesterification, so that the substrate was more likely to get close to the catalytic site and the specific activity of the lipase was improved by the AEAPS modified supports. It contributed to a large difference of activities between free and immobilized lipase. It has been reported that surface properties of the supports allowed effective interaction surrounding the catalytic site of lipase, and it contributed to the hyperactivation of lipase via interfacial activation, i.e. the formation of a suitable open structure for efficient contact with the substrates. The reusability of the immobilized enzyme was investigated and shown in Fig 10b, the

relative activity of lipase immobilized on RCMs and MRCMs was only 10.4 % and 29.7% after reuse for 5 times, respectively, while for the ARCM-2 and AMRCM1-2, the relative activity still remained 72.8% and 71.2% after reuse for 5 times, respectively. These results indicated an acceptable activity and reusability of the immobilized lipase on amino-modified magnetic cellulose microspheres for (R)-1-phenylethanol. It suggested that the amino groups introduced into the magnetic cellulose microsphere were effective for the immobilization of lipases. The difference in the activity would relate to the supports for the immobilized lipase, and it indicated that the surface properties of the supports had an important influence on the stability and activity of the immobilized lipase. The advantages of the AEAPS modified magnetic cellulose microsphere as a support over conventional materials included its excellent practical utility, in that it was lightweight, biocompatible and easy to handle. In particularly, the immobilized lipase on AEAPS modified magnetic cellulose microspheres was easily recovered and reused without significant decrease in a specific activity. Thus, the immobilization of lipase on AEAPS modified magnetic cellulose microspheres led to the improvement of activity and reusability for non-aqueous transesterification, without notable loss of selectivity.

Conclusions

Magnetic cellulose microsphere was modified with amino groups by using AEAPS successfully, and the obtained microspheres were used as supports for the immobilization of lipase. The immobilized lipase on the AEAPS-modified magnetic cellulose microspheres had an obviously increased catalytic activity. Furthermore,

the immobilized lipase on AEAPS modified magnetic cellulose microspheres was easily recovered and reused without significant decrease in the non-aqueous transesterification reaction. It suggested that the amino groups introduced into the magnetic cellulose microsphere were effective for the immobilization of lipases. The advantages of the magnetic microspheres over other supports were sustainability and biocompatibility with the enzyme, and the chemically modified magnetic cellulose microspheres was a green support material that provided both excellent practical utility and favorable reaction fields for enzymes and other catalysts. This type of biocompatible material was proposed to have promising potential in opening up numerous opportunities to take full advantage of magnetic cellulose microspheres in enzyme immobilization as results of their facile availability, cost-effective productivity, and excellent recoverable performance.

Acknowledgement

This work was supported by the National Natural Science Foundation of China (No. 51273085), and the Natural Science Foundation of Hubei Province (no. 2014CFB325), and project (2014PY024, 2662015PY099) by the Fundamental Research Funds for the Central Universities.

References

1 T. Mohan, R. Rathner, D. Reishofer, M. Koller, T. Elschner, S. Spirk, T. Heinze, K. Stana-Kleinschek, R. Kargl, *Biomacromolecul*, 2015, **16**, 2403-2411.

2 C. Wu, Y. Hu, M. Miller, R. V. Aroian, M. J. Sailor, *ACS Nano,* 2015, **9**, 6158-6167.

3 F. Shieh, S. Wang, C. Yen, C. Wu, S. Dutta, L. Chou, J. V. Morabito, P. Hu, M. Hsu, K. C.-W. Wu, C. Tsung, *J. Am. Chem. Soc*. 2015, **137**, 4276-4279.

4 E. Magner, *Chem. Soc. Rev*. 2013, **42**, 6213-6222.

5 A. S. Campbell, C. Dong, F. Meng, J. Hardinger, G. Perhinschi, N. Wu, C. Z. Dinu, *ACS Appl. Mater. Interfaces*. 2014, **6**, 5393-5403.

6 M. F. Vieira, A. M. S. Vieira, G. M. Zanin, P. W. Tardioli, C. Mateo, J. M. Guisán, *J. Mol. Catal B-Enzym*. 2011, **69**, 47-53.

7 R. Sato, T. Kawakami, H. Tokuyama, *React. Funct. Polym*. 2004, **76**, 8-12.

8 S. Cantone, V. Ferrario, L. Corici, C. Ebert, D. Fattor, P. Spizzoa, L. Gardossi, *Chem. Soc. Rev*. 2013,**42**, 6262-6276.

9 Q. Feng, D. Hou, Y. Zhao, T. Xu, T. J. Menkhaus, H. Fong, *ACS Appl. Mater. Interfaces*. 2014, **6**, 20958-20967.

10 K. Yao, P. Tan, Y. Luo, L. Feng, L. Xu, Z. Liu, Y. Li, R. Peng, *ACS Appl. Mater. Interfaces*. 2015, **7**, 12270-12277.

11 A. Karimi, A. Othman, A. Uzunoglu, L. Stanciu, S. Andreescu, *Nanoscale*. 2015, **7**, 6909-6923.

12 Z. Chen, J. Zhang, S. Singh, P. Peltier-Pain, J. S. Thorson, B. J. Hinds, *ACS Nano*. 2014, **8**, 8104-8112.

13 S. Wang, W. Chen, S. He, Q. Zhao, X. Li, J. Sun, X. Jiang, *Nanoscale*, 2014, **6**, 6468-6472.

14 X. Mu, J. Qiao, L. Qi, P. Dong, H. Ma, *ACS Appl. Mater. Interfaces*. 2014, **6**, 21346-21354.

15 J. Shi, S. Zhang, X. Wang , Z. Jiang, *Chem. Commun*. 2014, **50**, 12500-12503.

16 J. Shi, C. Yang, S. Zhang, X. Wang, Z. Jiang, W. Zhang, X. Song, Q. Ai，C. Tian, *ACS Appl. Mater. Interfaces*. 2013, **5**, 9991-9997.

17 M. Hartmann, X. Kostrov, *Chem. Soc. Rev*. 2013, **42**, 6277-6289.

18 J. Liu, Q. Yang, C. Li, *Chem. Commun*. 2015, **51**, 13731-13739.

19 H. Koga, T. Kitaoka, A. Isogai, *J. Mater. Chem*. 2012, **22**, 11591-11597.

20 Z. Liu, H. Wang, B. Li, C. Liu, Y. Jiang, G. Yu, X. Mu, *J. Mater. Chem*, 2012, **22**, 15085-15091.

21 C. Miao ,W. Y. Hamad, *Cellulose*, 2013, **20**, 2221-2262.

22 S. K. Ramamoorthy, M. Skrifvars, A. Persson, *Polym. Rev*, 2015, **55**, 107-162.

23 T. Rosenau, A. Hofinger, A. Potthast, P. Kosma, *Polymer*, 2003, **44**, 6153-6158.

24 E. Sjöholm, K. Gustafsson, B. Eriksson, W. Brown, A. Colmsjö, *Carbohyd. Polym*, 2000, **41**, 153-161.

25 L. Feng , Z. Chen, *J. Mol. Liq*, 2008, **142**, 1-5.

26 S. Liu, L. Zhang, J. Zhou, R. Wu, *J. Phys. Chem. C*, 2008, **112**, 4538-4544.

27 S. Liu, L. Zhang, J. Zhou, J. Xiang, J. Sun, J. Guan, *Chem. Mater*, 2008, **20**, 3623-3628.

28 S. Liu, J. Zhou, L. Zhang, *J. Phys. Chem. C*, 2011, **115**, 3602-3611.

29 S. Liu, T. Yu, Y. Wu, W. Li, B. Li, *RSC. Adv*, 2014, **4**, 34134-34143.

30 S. C. Lau, H. N. Lim, M. Basri, F. H. R. Masoumi, A. A. Tajudin, C. H. Chia, *Plos. One*, 2014, **9**, 0114093.

31 M. Koch Frings, W. Hartmeier, Enzyme. *Microb. Tech*, 1999, **25**, 303-309.

32 S. Shah, K. Solanki, M. N. Gupta, *Chem. Cent. J*, 2007, **1**, 30.

33 B. H. Sohn , R. E. Cohen, *Chem. Mater*, 1997, **9**, 264-269.

34 D. L. Leslie-Pelecky, R. D. Rieke, *Chem. Mater*, 1996, **8**, 1770-1783.

35 L. Zhang, G. Chen, H. Tang, Q. Cheng, S. Wang, *J. Appl. Polym. Sci*, 2009, **112**, 550-556.

36 W. Hu, S. Chen, Z. Yang, L. Liu, The *J. Phys. Chem. B*, 2011, **115**, 8453-8457.

37 C. Lin, M. Yang, H. Wei, *J. Power. Sources*, 2015, **282**, 562-571.

Table 1. Properties of the RCMs, MRCMs, RCMs treated with AEAPS and MRCMs treated with AEAPS. .

Sample	$CoFe_2O_4$ content (wt%)	Porosity (%)	S_{BET} (m^2/g)	Average diameter (μm)	Lipase amount mg	U/μmol product per min	Specific activity/ U per mg protein
Free lipase	--	--	--	--	17.0[a]	0.23	0.013
RCM	--	97 ± 5	109	281 ± 2.3	0.195	0.028	0.143
MRCM-1	4.63	96 ± 4	97	278 ± 1.8	0.330	0.031	0.094
MRCM-2	7.79	96 ± 8	79	273 ± 1.7	0.327	0.028	0.086
MRCM-3	11.32	96 ± 5	75	275 ± 1.8	0.563	0.027	0.048
MRCM-4	15.28	95 ± 8	66	273 ± 2.4	0.313	0.016	0.051
ARCM-1	--	70 ± 5	48	277 ± 7.2	1.580	0.63	0.399
ARCM-2	--	67 ± 4	46	235 ± 5.4	1.742	0.79	0.453
ARCM-3	--	65 ± 5	58	287± 8.6	1.387	0.57	0.411
AMRCM1-1	4.63	67 ± 3	53	288 ± 5.8	1.292	0.50	0.387
AMRCM1-2	4.63	64 ± 4	50	301 ± 4.8	1.512	0.63	0.417
AMRCM1-3	4.63	63 ± 3	50	312 ± 3.6	1.330	0.51	0.383

a, the mass of the free lipase used.

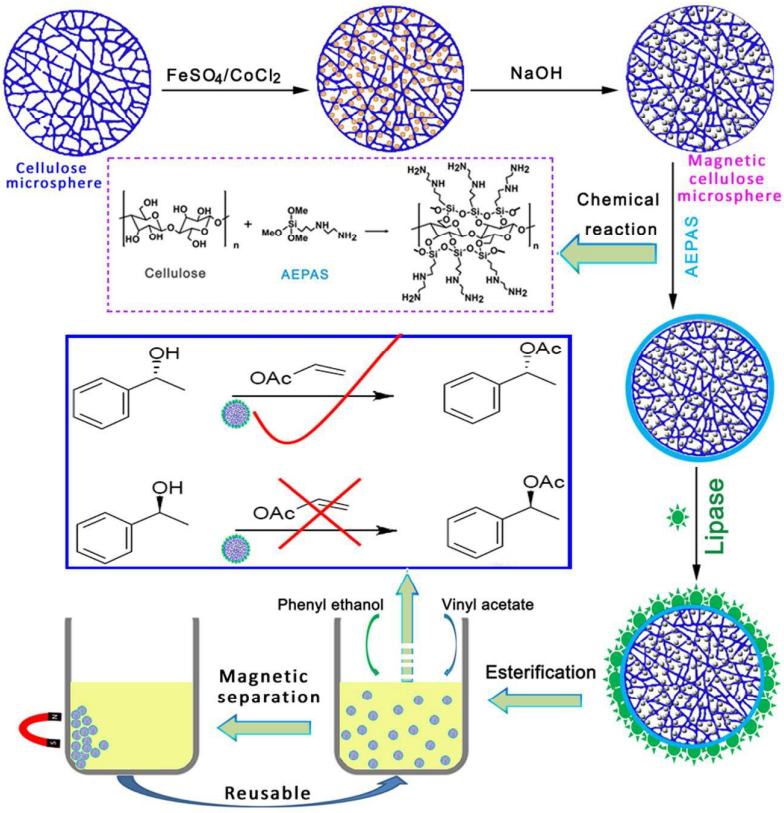

Scheme 1. Schematic illustration of synthesis strategy for ARCMs, the enzyme immobilization onto AMRCMs, their catalysis and reusability.

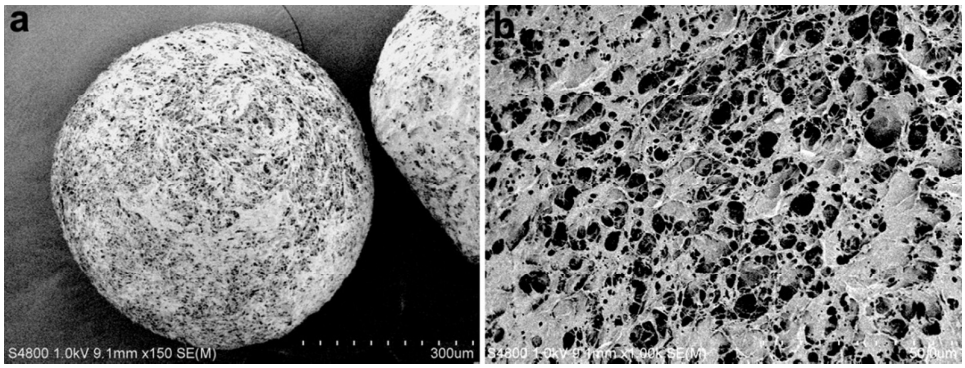

Fig 1. SEM images of the surface morphology of the regenerated cellulose microspheres.

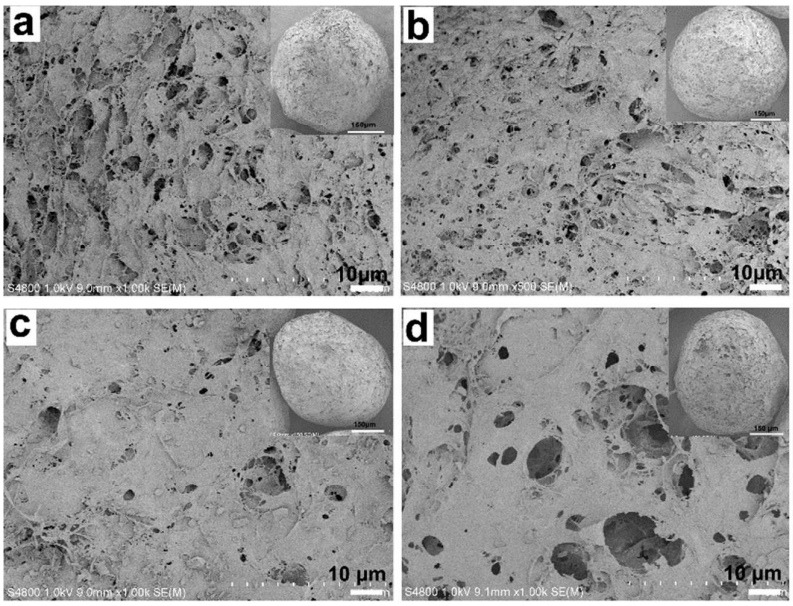

Fig 2. SEM images of the surface morphology of the magnetic regenerated cellulose microspheres, a, b, c, d were for MRCM-1, MRCM-2, MRCM-3 and MRCM-4, respectively

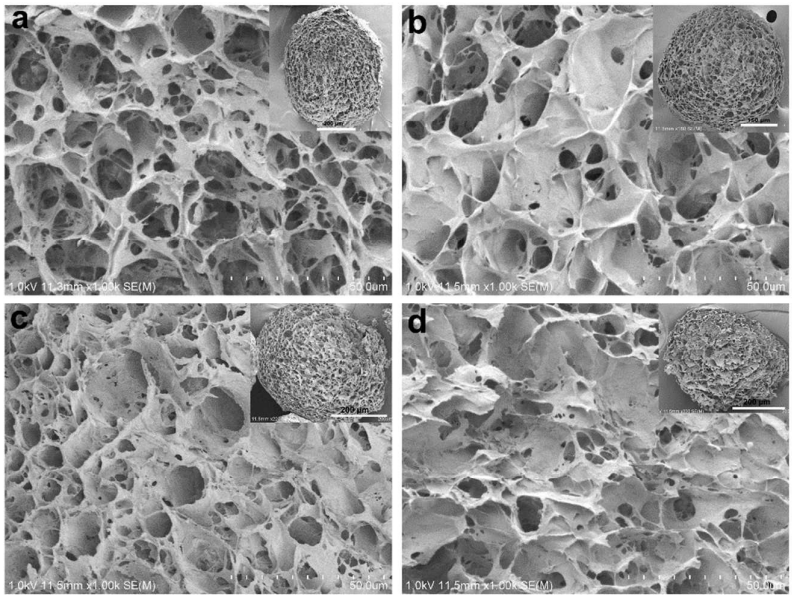

Fig 3. SEM images of the cross-section morphology of the magnetic regenerated cellulose microspheres, a, b, c, d were for MRCM-1, MRCM-2, MRCM-3 and MRCM-4, respectively.

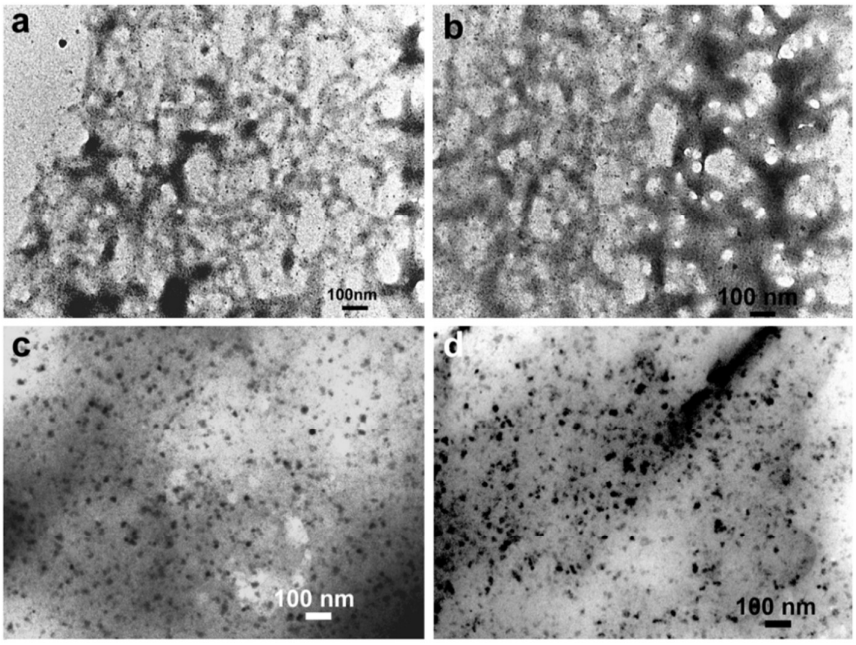

Fig 4. TEM images of magnetic nanoparticles, a, b, c, d were MRCM-1, MRCM-2, MRCM-3 and MRCM-4, respectively.

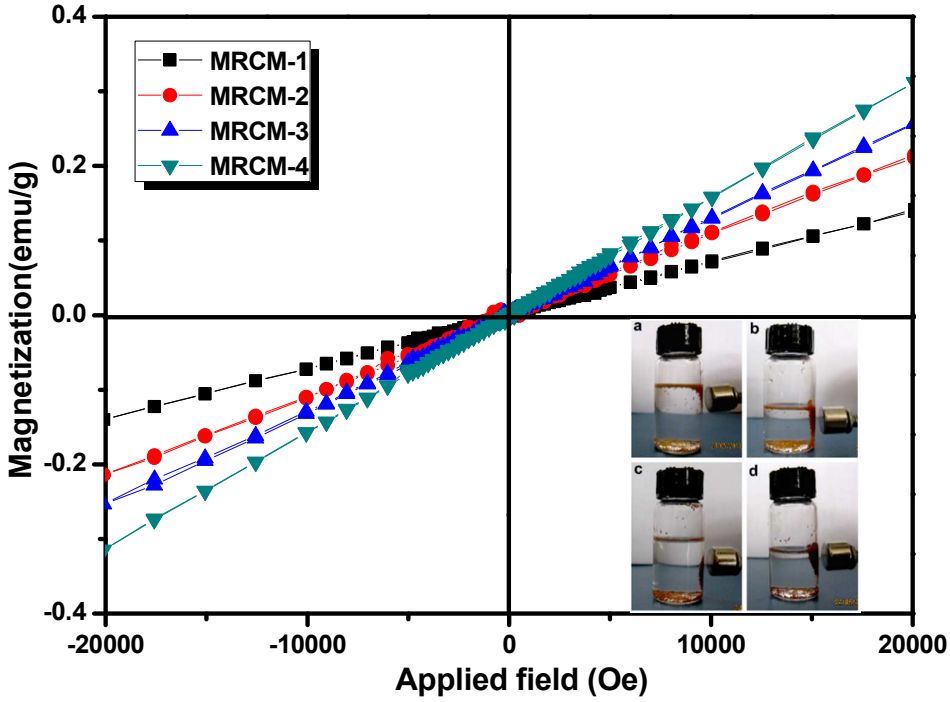

Fig 5. The magnetic hysteresis loop of the magnetic regenerated cellulose microspheres at 298 k, and the inset photos were for the MRCM-1 (a), MRCM-2 (b), MRCM-3 (c) and MRCM-4 (d) in H_2O under a magnetic field.

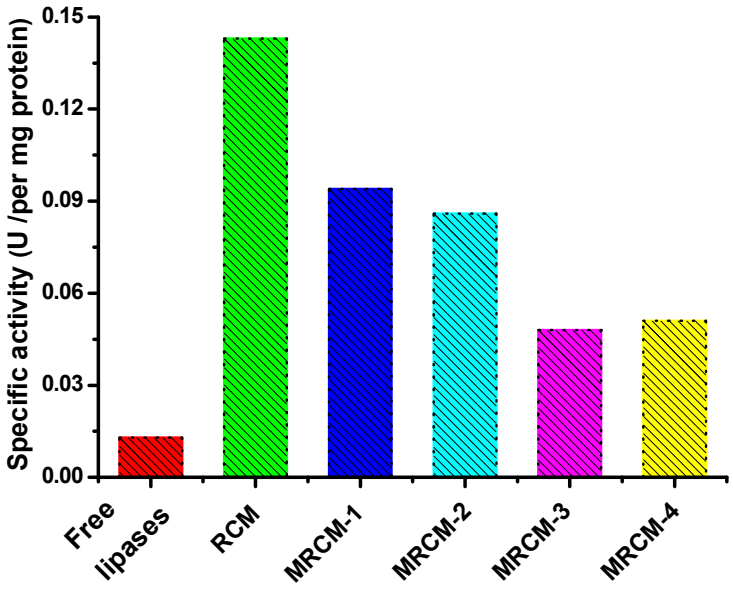

Fig 6. The specific activities of the lipase enzymes without immobilization and immobilized on the cellulose microspheres, magnetic cellulose microspheres and AEPAS modified magnetic cellulose microspheres.

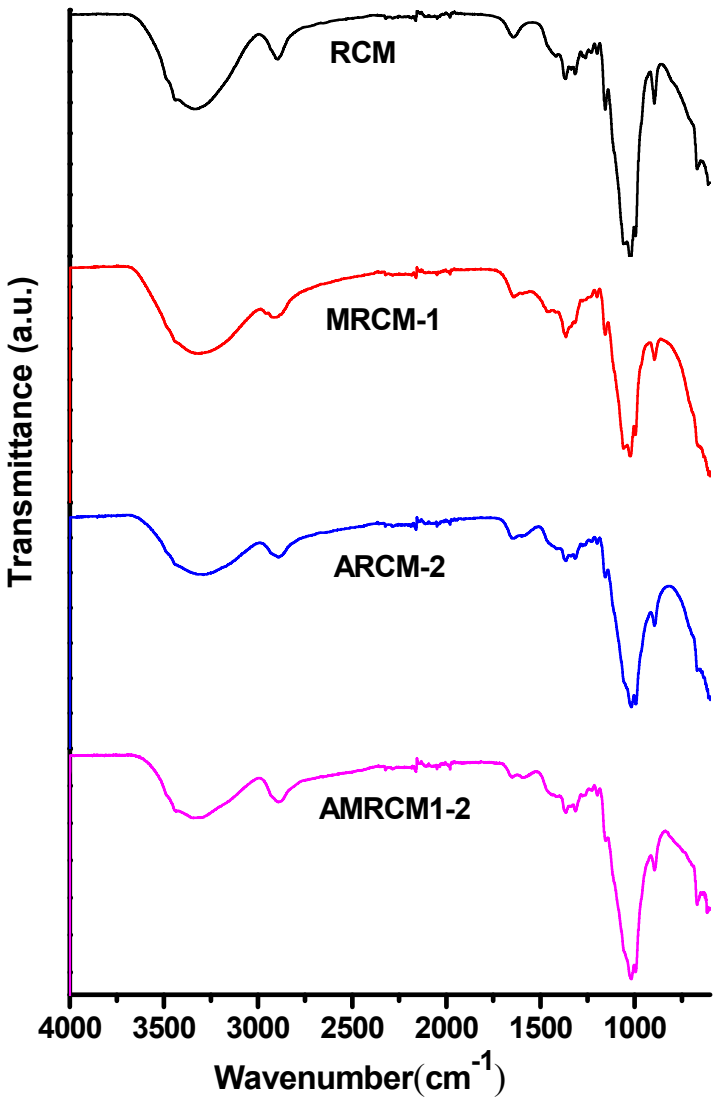

Fig 7. FT-IR of the pristine cellulose and magnetic cellulose microsphers with and without modification with AEAPS.

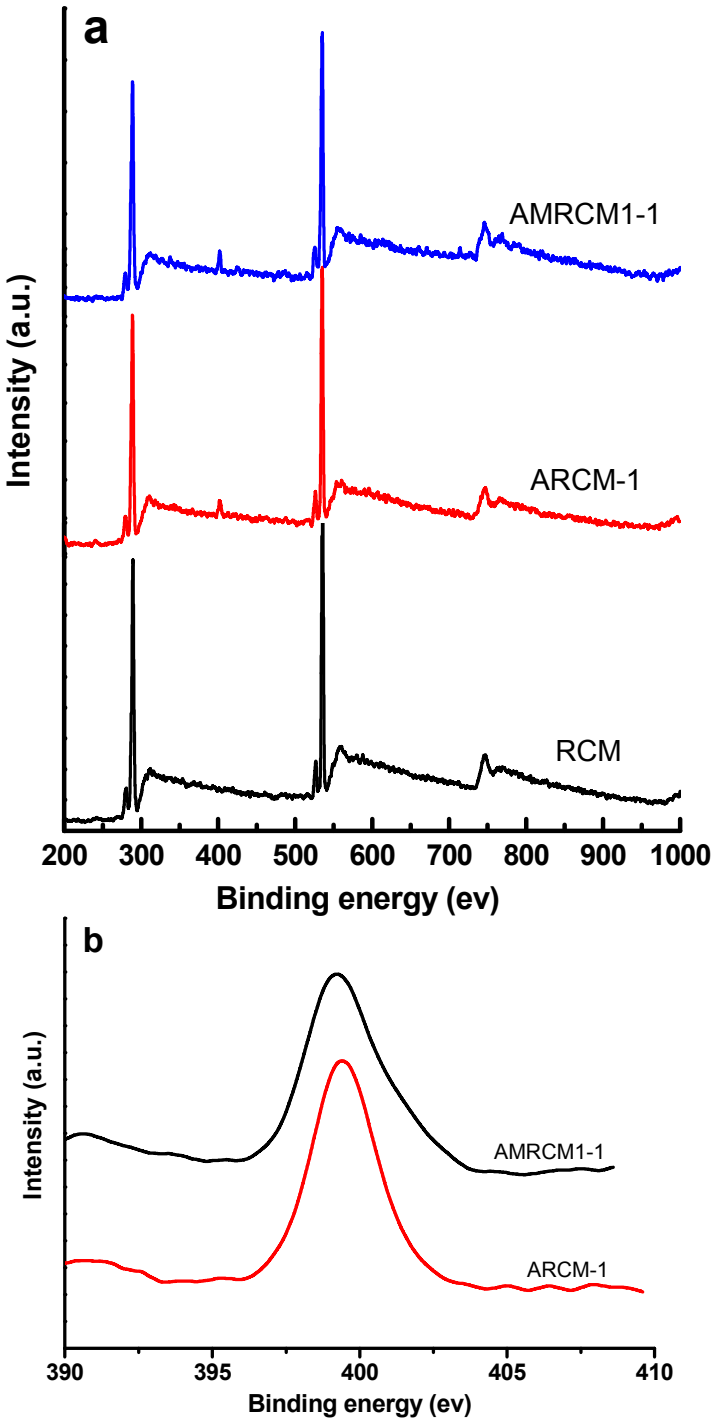

Fig 8. XPS spectra for the RCM, ARCM-1, and ARCM1-1.

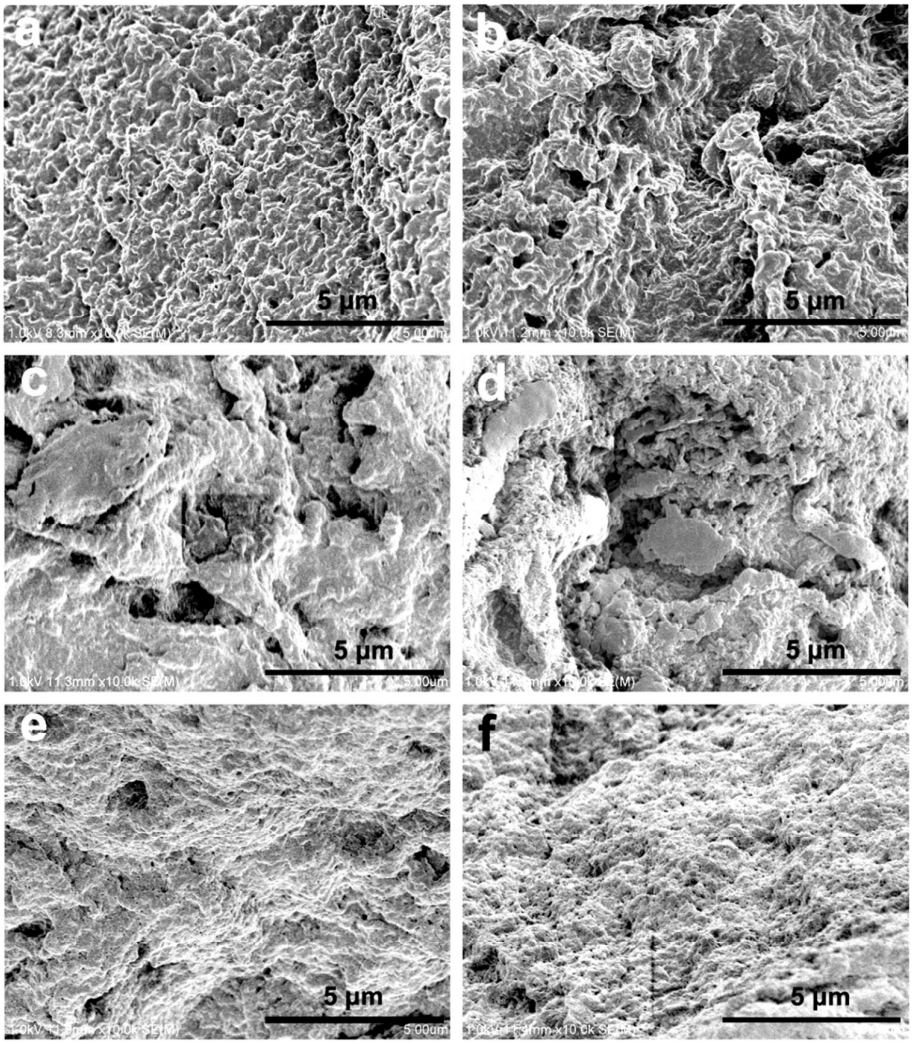

Fig 9. SEM images of cellulose microspheres and magnetic cellulose microspheres (MRCM-1) after being modified by using AEAPS, a, b, c, d, e, f were for ARCM-1, ARCM-2, ARCM-3, ARCM1-1, ARCM1-2, ARCM1-3, respectively.

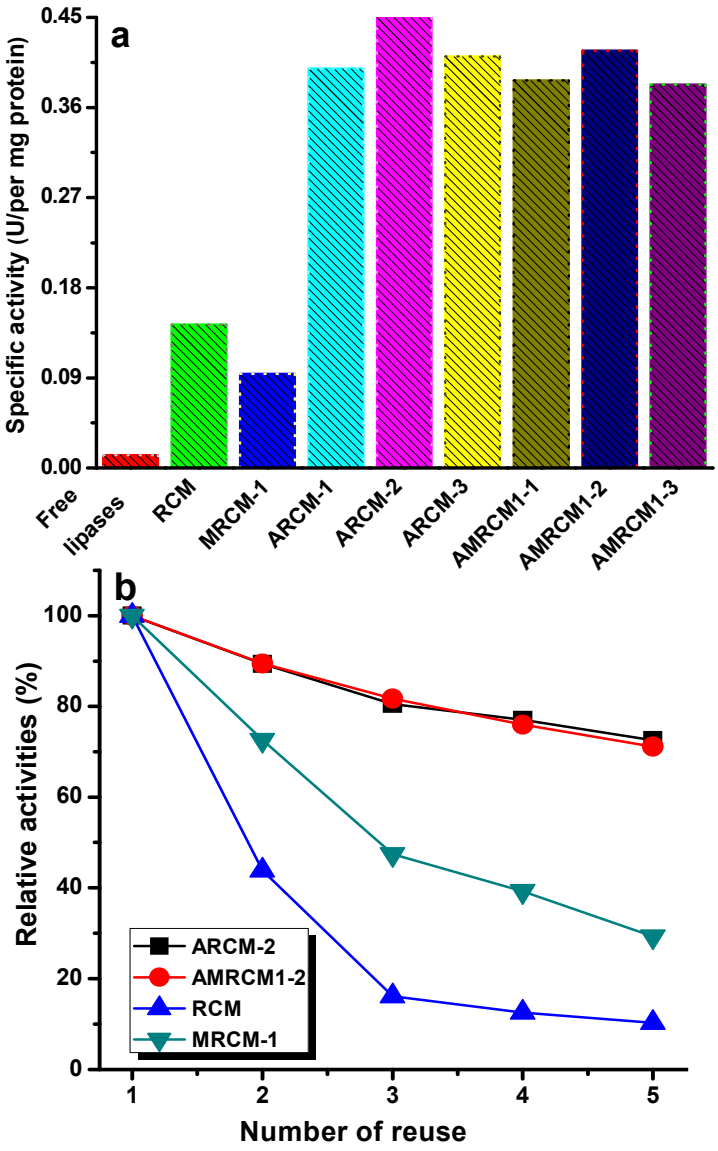

Fig 10. (a) Effect of the lipases amount on the activity of immobilized lipases in ARCMs-2 and (b) reusability performance of immobilized lipases RCM, ARCM-2, MRCM-1 and AMRCM1-2 in repeated reaction.

For table of content use only